VIH2 Regulates the Synthesis of Inositol Pyrophosphate InsP$_8$ and Jasmonate-Dependent Defenses in Arabidopsis[OPEN]

Debabrata Laha,[a] Philipp Johnen,[a,1] Cristina Azevedo,[b,1] Marek Dynowski,[c] Michael Weiß,[d] Samanta Capolicchio,[e] Haibin Mao,[f] Tim Iven,[g] Merel Steenbergen,[h] Marc Freyer,[a] Philipp Gaugler,[a] Marília K.F. de Campos,[a] Ning Zheng,[f] Ivo Feussner,[g] Henning J. Jessen,[e] Saskia C.M. Van Wees,[h] Adolfo Saiardi,[b] and Gabriel Schaaf[a,2]

[a] Center for Plant Molecular Biology, University of Tübingen, 72076 Tübingen, Germany
[b] Medical Research Council Laboratory for Molecular Cell Biology, University College London, London WC1E 6BT, United Kingdom
[c] Zentrum für Datenverarbeitung, University of Tübingen, 72074 Tübingen, Germany
[d] Department of Biology, University of Tübingen, 72076 Tübingen, Germany
[e] Department of Chemistry, University of Zürich, 8057 Zurich, Switzerland
[f] Department of Pharmacology, Howard Hughes Medical Institute, University of Washington, Seattle, Washington 98195
[g] Department of Plant Biochemistry, Georg-August-University Göttingen, 37077 Göttingen, Germany
[h] Plant-Microbe Interactions, Department of Biology, Utrecht University, 3508 TB Utrecht, The Netherlands

ORCID IDs: 0000-0002-7823-5489 (D.L.); 0000-0002-4512-9508 (P.J.); 0000-0002-1025-9484 (H.J.J.); 0000-0001-9022-4515 (G.S.)

Diphosphorylated inositol polyphosphates, also referred to as inositol pyrophosphates, are important signaling molecules that regulate critical cellular activities in many eukaryotic organisms, such as membrane trafficking, telomere maintenance, ribosome biogenesis, and apoptosis. In mammals and fungi, two distinct classes of inositol phosphate kinases mediate biosynthesis of inositol pyrophosphates: Kcs1/IP6K- and Vip1/PPIP5K-like proteins. Here, we report that PPIP5K homologs are widely distributed in plants and that *Arabidopsis thaliana* VIH1 and VIH2 are functional PPIP5K enzymes. We show a specific induction of inositol pyrophosphate InsP$_8$ by jasmonate and demonstrate that steady state and jasmonate-induced pools of InsP$_8$ in Arabidopsis seedlings depend on VIH2. We identify a role of VIH2 in regulating jasmonate perception and plant defenses against herbivorous insects and necrotrophic fungi. In silico docking experiments and radioligand binding-based reconstitution assays show high-affinity binding of inositol pyrophosphates to the F-box protein COI1-JAZ jasmonate coreceptor complex and suggest that coincidence detection of jasmonate and InsP$_8$ by COI1-JAZ is a critical component in jasmonate-regulated defenses.

INTRODUCTION

Inositol polyphosphates became an intense focus of research with the discovery that *myo*- inositol 1,4,5-trisphosphate (InsP$_3$) mobilizes Ca^{2+} in a receptor-dependent fashion from intracellular stores in pancreatic cells (Streb et al., 1983). The stereochemistry of D-*myo*-inositol suggested that the inositol ring represents a 6-bit signaling scaffold with the potential to "encode" 64 unique signaling states (York, 2006). In plants, InsP$_3$ has been associated with a wide range of cellular functions, such as guard cell physiology (Blatt et al., 1990; Gilroy et al., 1990; Burnette et al., 2003; Han et al., 2003), drought tolerance (Knight et al., 1997; Perera et al., 2008), heat shock responses (Liu et al., 2006), blue light perception (Chen et al., 2008), root gravitropism (Wang et al., 2009; Zhang et al., 2011), response to mechanical wounding (Mosblech et al., 2008), and pollen dormancy (Y. Wang et al., 2012). However, the role of InsP$_3$ and other inositol phosphates in

plant signaling remains controversial as no inositol phosphate receptor has been identified to date (Munnik and Vermeer, 2010; Munnik and Nielsen, 2011; Gillaspy, 2013).

Recent discoveries that InsP$_6$ binds to the auxin receptor complex TIR1/IAA (Tan et al., 2007) and InsP$_5$ binds to the jasmonate receptor complex COI1/JAZ (Sheard et al., 2010) suggest that inositol polyphosphates are involved in plant hormone perception. COI1 is the F-box component of a SKP1-CUL1-F-box protein (SCF) ubiquitin E3 ligase complex that recruits Jasmonate ZIM-domain (JAZ) transcriptional repressors upon binding to the bioactive jasmonic acid (JA) conjugate JA-Ile. This triggers polyubiquitylation and subsequent degradation of the JAZ repressors by the 26S proteasome (Chini et al., 2007; Thines et al., 2007; Katsir et al., 2008; Sheard et al., 2010). JAZ degradation relieves repression of *MYC2* and other transcription factors, thus permitting the expression of jasmonate-responsive genes (Chini et al., 2007). Mass spectrometry and NMR analyses revealed that inositol-1,2,4,5,6-pentakisphosphate [Ins(1,2,4,5,6)P$_5$] copurified with Arabidopsis SKP1 homolog (ASK1)-COI1 expressed in insect cells (Sheard et al., 2010). Although ligand binding based reconstitution assays suggested that Ins(1,2,4,5,6)P$_5$ potentiates jasmonate receptor assembly in vitro, its physiological role remains unclear. Two studies that analyzed *Arabidopsis thaliana* backgrounds altered in inositol polyphosphate metabolism provide evidence that this class of molecules contributes to COI1
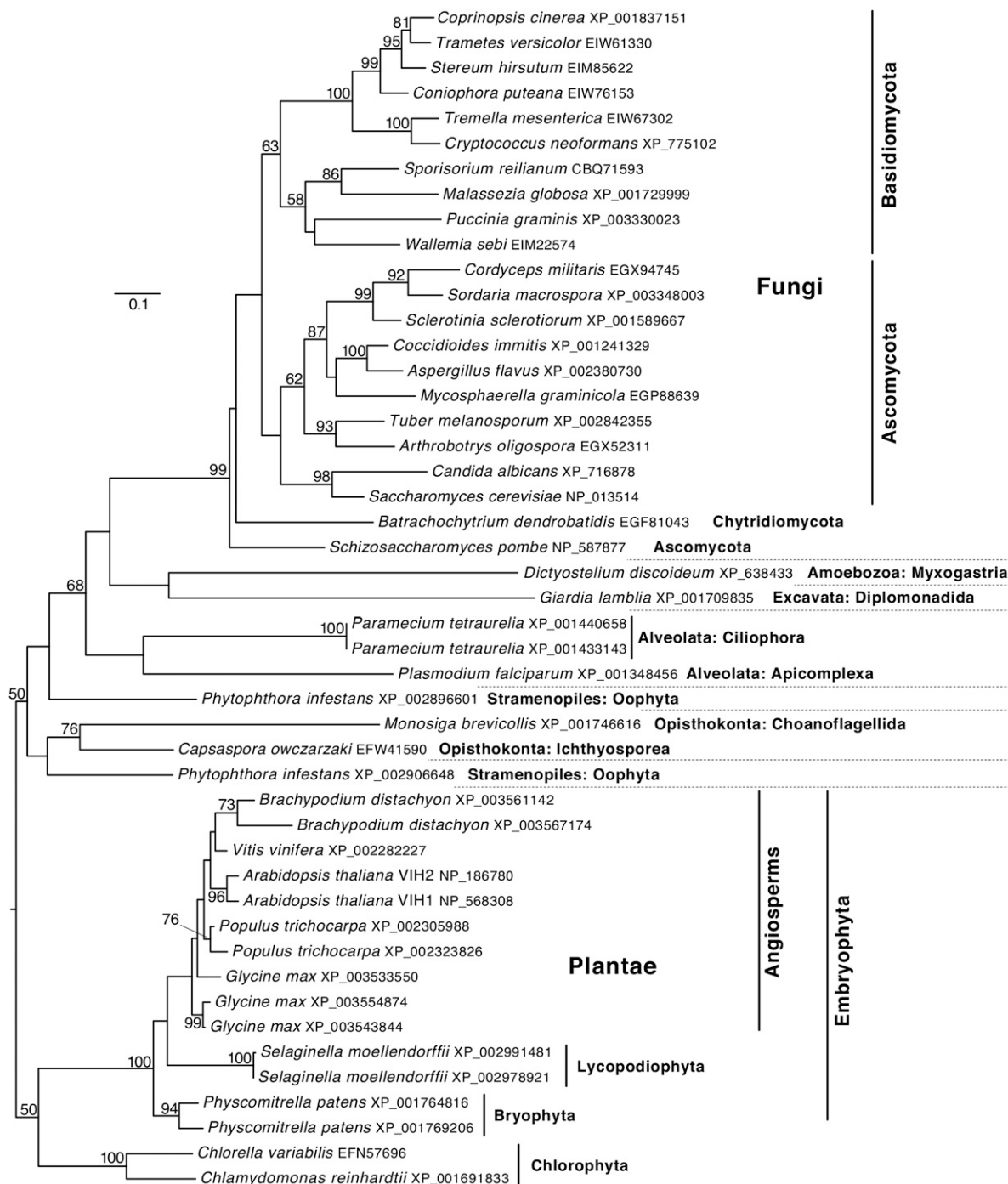
Figure 1. Vip1/PPIP5K Homologs Are Ubiquitous in Plants.

BLAST search analyses were performed employing the protein sequence of the *Saccharomyces cerevisiae* Vip1 ATP-grasp kinase domain (residues 1 to 535) as a search template. The tree was estimated from an alignment of ATP-grasp kinase domains of the encoded proteins using maximum likelihood. Branch support was calculated from 10,000 bootstrap replicates, and values below 50% are omitted. Branch lengths are given in terms of expected numbers of amino acid substitutions per site.
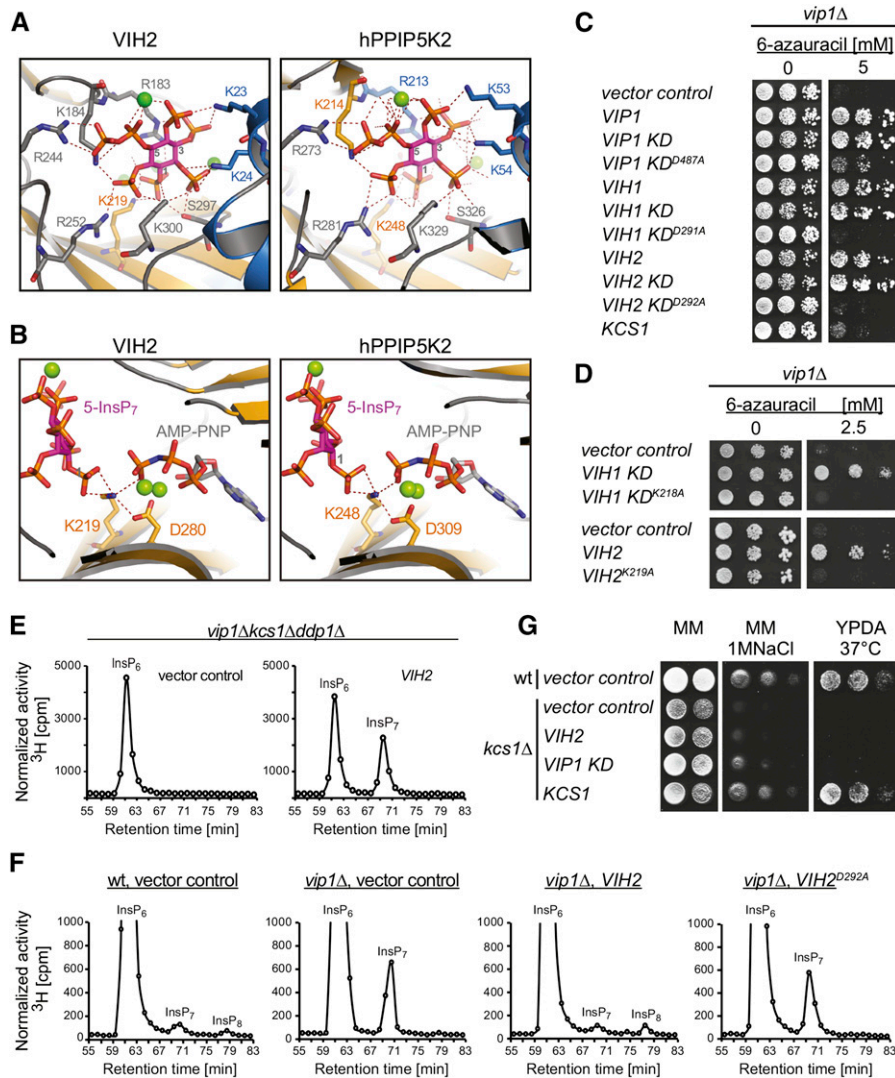
Figure 2. VIH1 and VIH2 Are Functional Vip1-Type PPIP5 Kinases.

(A) and **(B)** Structural model of the VIH2 ATP-grasp kinase domain (left) and the hPPIP5K2 ATP-grasp kinase domain (PDB ID: 3T9D, right) depicting the 5-InsP$_7$ binding sites and key catalytic residues. Residues coordinating substrate via polar contacts are shown as sticks, polar interactions are highlighted by dashed lines, α-helices are rendered in blue, β-sheets in orange, substrate (5-InsP$_7$) is rendered in magenta, and Mg^{2+} ions are presented as green spheres. Three carbon atoms on the inositol ring are numbered. The ATP analog AMP-PNP (in **[B]**) is depicted with gray carbon and orange and red phosphate groups.

(C) and **(D)** Complementation of *vip1Δ*-associated growth defects in yeast by ectopic expression of inositol pyrophosphate synthetases. The *vip1Δ* yeast strain transformed with episomal pDR195(*URA3*) plasmids carrying either *VIP1*, *VIH1*, or *VIH2*, sequences encoding their respective ATP-grasp kinase domains (*KD*) or designated kinase domain mutants, or carrying *KCS1* were spotted in 8-fold serial dilutions onto uracil-free minimal medium in presence or absence of 6-azauracil, as indicated. Rescue on medium supplemented with 6-azauracil (right) reports Vip1 activity.

(E) and **(F)** Normalized HPLC profiles of inositol phosphates of extracts from designated [^{3}H] inositol-labeled yeast transformants. Extracts were resolved by Partisphere SAX HPLC and fractions collected each minute for subsequent determination of radioactivity as indicated. Changes in elution times in independent experiments were observed and can be explained by subtle changes in column properties or column change. Experiments were repeated three times with similar results.

(G) Complementation assays of *kcs1Δ*-associated growth defects on high salt by ectopic expression inositol pyrophosphate synthetases. Wild-type (wt) or *kcs1Δ* yeast transformants (both DDY1810 background) carrying designated plasmids were spotted in 8-fold serial dilutions onto solid minimal media (MM, uracil deficient CSM media with YNB and appropriate supplements) in presence or absence of NaCl and onto solid YPDA media incubated at 37°C.

function during the plants wound response (Mosblech et al., 2008, 2011).

The discovery of diphosphoinositol polyphosphates, also referred to as inositol pyrophosphates, in amoebae, mammals, and yeast (Stephens et al., 1991; Menniti et al., 1993; Saiardi et al., 2000b) revealed an even higher complexity of this family of signaling molecules. In these organisms, inositol pyrophosphates regulate many cellular processes, including stress responses, membrane trafficking, telomere maintenance, ribosome biogenesis, cytoskeletal dynamics, insulin signaling, apoptosis, phosphate homeostasis, and neutrophil activation (Barker et al., 2009; Burton et al., 2009; Shears, 2009; Chakraborty et al., 2011; Wundenberg and Mayr, 2012). Two distinct classes of inositol pyrophosphate synthetases have been described: inositol hexakisphosphate kinases (also termed IP6Ks or Kcs1-like proteins) and diphosphoinositol pentakisphosphate kinases (PPIP5K or IP7K/Vip1-like proteins). IP6Ks phosphorylate the phosphate in the 5-position of $InsP_6$ and $Ins(1,3,4,5,6)P_5$ ($InsP_5$) and can use the resulting inositol pyrophosphates as substrates to generate more complex molecules containing two or more additional pyrophosphate moieties (Saiardi et al., 2000a, 2001; Draskovic et al., 2008). In contrast, PPIP5Ks phosphorylate the phosphate in the 1-position of both 5-$InsP_7$ and $InsP_6$, leading to the formation of the $InsP_8$ isomer $1,5(PP)_2$-$InsP_4$ (1,5-$InsP_8$) and the $InsP_7$ isomer 1PP-$InsP_5$ (1-$InsP_7$), respectively (Mulugu et al., 2007; Lin et al., 2009; H. Wang et al., 2012).

The existence of inositol species more polar than $InsP_6$ has been reported in *Spirodela polyrrhiza* (Flores and Smart, 2000), barley (*Hordeum vulgare*; Brearley and Hanke, 1996; Dorsch et al., 2003), guard cells of intact guard cells of potato (*Solanum tuberosum*; Lemtiri-Chlieh et al., 2000), and in extracts of Arabidopsis and maize (*Zea mays*; Desai et al., 2014). In the later study, the authors addressed a possible involvement of Arabidopsis Vip1 homologs in the synthesis of inositol pyrophosphates by performing yeast complementation assays (Desai et al., 2014). Based on these assays, the authors proposed a function of Arabidopsis Vip1 homologs as IP6K enzymes with a possible role in $InsP_7$ biosynthesis. However, plants with altered Vip1 functions have not been investigated and the physiological role(s) of Vip1 proteins and inositol pyrophosphates in plants await clarification.

Here, we show that plant genomes of phylogenetically diverse taxa encode Vip1 homologs that appear to have evolved from a single common ancestor. We also provide evidence that $InsP_7$ and $InsP_8$ are readily detected in Arabidopsis extracts. The Vip1 homologs VIH1 and VIH2 are functional PPIP5Ks, and VIH2 is critical for $InsP_8$ production in Arabidopsis seedlings. Our data further suggest that VIH2-dependent inositol pyrophosphates represent key cofactors of the COI1-JAZ receptor complex, thereby playing an important role in jasmonate perception and jasmonate-regulated defenses.

Note that in a previous published work (Desai et al., 2014), which was published during the preparation of this article, Arabidopsis homologs of yeast Vip1 were named AtVIP1 and AtVIP2 (corresponding to VIH2 and VIH1, respectively). Because VIP1 is already in use for an unrelated protein (Arabidopsis VirE2 Interacting Protein 1, encoded by At1g43700), we propose to use the gene symbol *VIH* (*VIP1* homolog) registered at the TAIR database (see http://www.arabidopsis.org).

RESULTS

### Vip1/PPIP5K Homologs Are Widespread in Plants

BLAST searching with the N-terminal ATP-grasp kinase domain of Vip1 as the query sequence allowed us to identify genes encoding putative Vip1/PPIP5K proteins in all available plant genomes, including diverse taxa such as green algae (Chlorophyta), mosses (Bryophyta), lycopods, and monocot and eudicot angiosperms, suggesting that PPIP5Ks play important basic functions in all plants. Phylogenetic analysis of the N-terminal ATP-grasp kinase domain of selected proteins, with a focus on plants and fungi, reflects major monophyletic groups as currently accepted (Keeling et al., 2009; Blackwell et al., 2012) (Figure 1). According to the maximum likelihood tree (Figure 1), all of the plant homologs are derived from a single ancestral gene, with subsequent gene duplications in the individual lineages.

The N-Terminal ATP-Grasp Kinase Domain in Arabidopsis Vip1 Homologs Has a Two-Domain Architecture and Is Structurally Conserved

We named the Arabidopsis Vip1 homologs identified in our BLAST search VIH1 and VIH2 (Vip1 homolog), respectively. Protein sequence comparison suggests that both proteins possess a two-domain architecture conserved in members of the Vip1/PPIP5K family, with an N-terminal ATP-grasp kinase domain and a C-terminal phosphatase-like domain (Supplemental Figure 1A). A model of the VIH2 kinase domain based on the crystal structure of human diphosphoinositol pentakisphosphate kinase 2 (hPPIP5K2) predicts the nucleotide analog AMP-PNP to be coordinated between two sets of antiparallel β-sheets as it has been described for hPPIP5K2 (H. Wang et al., 2012) (Supplemental Figure 1B). $InsP_7$ is coordinated exclusively by VIH2 lysine and arginine residues with the exception of one serine residue (as in hPPIP5K2), a hallmark of PPIP5K enzymes (H. Wang et al., 2012). Importantly, all protein-substrate interactions, including residues involved in the phosphotransfer reaction are conserved: VIH2 (hPPIP5K2) residues that coordinate the substrate are Lys-23 (Lys-53), Lys-24 (Lys-54), Arg-183 (Arg-213), Lys-184 (Lys-214), Lys-219 (Lys-248), Arg-244 (Arg-273), Arg-252 (Arg-281), Ser-297 (Ser-326), and Lys-300 (Lys-329) (Figures 2A and 2B) (H. Wang et al., 2012). These residues are also conserved in the VIH1 polypeptide (Supplemental Figure 1C). Collectively, these results suggest Arabidopsis VIH proteins execute Vip1/PPIP5K-like activities.

VIH1 and VIH2 Complement *vip1*Δ- but Not *kcs1*Δ-Associated Defects in Yeast

To address the function of VIH more directly, we investigated consequences of heterologous VIH expression in yeast. A previously identified *vip1*Δ-associated growth defect on 6-azauracil in yeast (Osada et al., 2012) was rescued by Arabidopsis VIH1 and VIH2, suggesting that these proteins execute Vip1-like activities in vivo (Figure 2C). In contrast, ectopic overexpression of Kcs1 under similar conditions failed to cause growth complementation of the single *vip1*Δ strain (Figure 2C). Rescue of this yeast strain was also observed by expression of the N-terminal
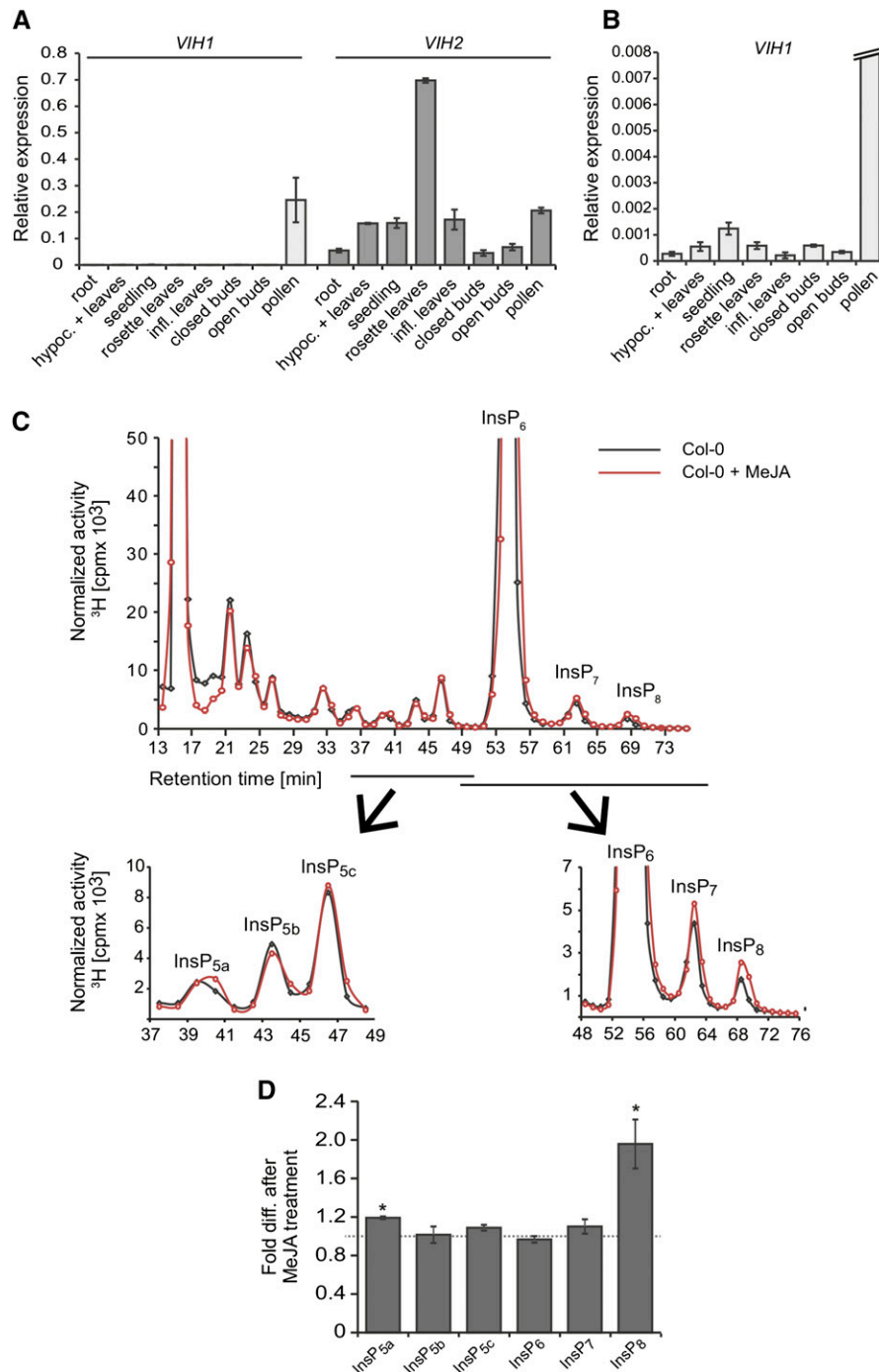
Figure 3. Expression Analyses Suggest Specialized Functions of *VIH1* and *VIH2*, and Inositol Pyrophosphates Can Be Detected in Arabidopsis Extracts and Are Regulated by Jasmonate.

(A) and **(B)** qPCR analyses of *VIH* expression in Col-0 plants using cDNA prepared from RNA extracts of different plant tissues as indicated. Averages of triplicate reactions ± sd are shown. β-*TUBULIN* was used as reference gene. Transcript levels of *VIH1* and *VIH2* are presented relative to β-*TUBULIN* transcript. The experiment was repeated three times with similar results.

(C) and **(D)** MeJA increases InsP$_8$ level. Normalized HPLC profiles **(C)** of 3-week old [^{3}H] inositol-labeled Col-0 seedlings that were untreated (solid gray line) or treated for 4 h with 50 μM MeJA (solid red lines). Treated and nontreated plants were harvested simultaneously to avoid daytime-dependent differences in inositol polyphosphate homeostasis. The experiment was repeated with similar results, and representative results from one experiment are shown. For relative amounts of respective species **(D)**, averages of fold differences after MeJA treatment of three independent experiments ± se are

kinase domains of Vip1, VIH1, and VIH2, indicating that the 6-azauracil sensitivity of $vip1\Delta$ is caused by loss of Vip1 kinase activity and, importantly, that VIH1 and VIH2 possess a functional Vip1-like ATP-grasp kinase domain. This idea is supported by the finding that kinase catalytic dead mutant Vip1^{D487A} (Mulugu et al., 2007) and the corresponding mutant proteins VIH1^{D291A} and VIH2^{D292A} failed to rescue $vip1\Delta$-associated growth defects on 6-azauracil (Figure 2C). In the context of the hPPIP5K2 enzyme, another residue, Lys-248, interacts with both the 1-phosphate of 5-InsP$_7$ and the γ-phosphate of ATP and therefore plays an essential function in the catalytic cycle of 5-InsP$_7$ phosphorylation and the specificity of the phosphotransfer reaction (Figure 2B) (H. Wang et al., 2012). This residue is conserved in plant Vip1 homologs and our structural model suggests that the corresponding Arabidopsis VIH2 residue K219 interacts with substrate and cofactor in a similar manner (Figure 2B).

In agreement with this idea, mutant polypeptides VIH1-KD^{K218A} and VIH2^{K219A} are dysfunctional (Figure 2D). All proteins, including catalytic dead mutants, were correctly expressed (Supplemental Figures 2A and 2B). We further investigated consequences of VIH2 expression on inositol polyphosphate metabolism in different yeast strains. We expressed VIH2 in a $vip1\Delta\ kcs1\Delta\ ddp1\Delta$ triple mutant yeast strain, which lacks inositol pyrophosphates and is devoid of Ddp1 (diadenosine-and-diphosphoinositol-polyphosphate-phosphohydrolase)-dependent inositol pyrophosphatase activity, thus facilitating the detection of inositol pyrophosphates synthesized by ectopically expressed kinases (Safrany et al., 1998; Mulugu et al., 2007). VIH2 expression in this background resulted in a robust InsP$_7$ peak that eluted at a retention time identical to the 1-InsP$_7$ peak in transformants ectopically expressing Vip1 (Figure 2E; Supplemental Figure 2D), supporting recent observations by Desai et al. (2014). However, these results did not address whether VIH proteins have Vip1/PPIP5K or Kcs1/IP6K-like activities.

Therefore, we expressed VIH2 in single $vip1\Delta$ or $kcs1\Delta$ mutant backgrounds. Because of a preference of Vip1 to phosphorylate 5-InsP$_7$ to 1,5-InsP$_8$, $vip1\Delta$ yeast cells accumulate the non-metabolized substrate 5-InsP$_7$ (Azevedo et al., 2009; Onnebo and Saiardi, 2009; Padmanabhan et al., 2009) (Figure 2F). Levels of 1-InsP$_7$ and 1,5-InsP$_8$ are generally low in wild-type yeast due to the activity of Ddp1 (Safrany et al., 1998; Mulugu et al., 2007). As apparent from a robust rescue of (i.e., decrease in) 5-InsP$_7$ levels, expression of VIH2 complemented $vip1\Delta$-associated defects in inositol pyrophosphate homeostasis in a kinase-dependent manner (Figure 2F; Supplemental Figure 2C). We also investigated the consequences of ectopic expression of Kcs1, Vip1, and VIH2 in a $kcs1\Delta$ single mutant yeast strain. While ectopic expression of Kcs1 complemented a previously described growth defect of $kcs1\Delta$ cells on 1 M NaCl at 37°C, ectopic expression of Vip1 and VIH2 under similar conditions failed to do so. This is in agreement

with the idea that VIH2 does not have Kcs1/IP6K-like activities (Figure 2G). We also found that overexpression of Vip1 kinase activity in $kcs1\Delta$ cells causes production of InsP$_7$ and InsP$_8$ (Supplemental Figure 2E). Based on previous in vitro studies (Losito et al., 2009), these species are likely to represent 1-InsP$_7$ and 1,3-InsP$_8$ or 1PPP-InsP$_7$. Likewise, ectopic expression of VIH2 caused peaks with identical chromatographic mobilities (Supplemental Figure 2E). Collectively, these data suggest that VIH2 executes Vip1/PPIP5K but not Kcs1/IP6K-like activities in yeast.

## Levels of the Inositol Pyrophosphate InsP$_8$ Are Regulated by Methyl Jasmonate and Depend on VIH2

Quantitative PCR (qPCR) analyses showed expression of *VIH1* to be restricted mainly to pollen (Figures 3A and 3B). *VIH2* expression, on the other hand, was ubiquitous and especially strong in rosette leaves (Figure 3A), suggesting specialized functions of both isoforms. To investigate VIH2 functions in planta, we analyzed inositol polyphosphates in 3-week-old seedlings of wild-type (Columbia-0 [Col-0]) and *vih2* mutant plants. HPLC runs of [^{3}H]-inositol-labeled Col-0 plant extracts showed a similar profile as reported previously (Stevenson-Paulik et al., 2005), with a robust peak at a retention time identical to the [^{3}H]-InsP$_6$ standard (Figure 3C; Supplemental Figure 3A). However, in contrast to this previous report, we also detected two additional peaks more anionic than InsP$_6$ that eluted at elution times expected for InsP$_7$ and InsP$_8$, respectively (Figure 3C), supporting recent findings by Desai et al. (2014).

Inositol phosphates have been implicated in the wound response (Mosblech et al., 2008, 2011; Sheard et al., 2010), a process that is regulated by the oxylipin JA and related signaling molecules (collectively referred to as jasmonates), as well as by the stress hormone abscisic acid (ABA) (Vos et al., 2013). Therefore, we explored the role of jasmonates and ABA in the regulation of inositol pyrophosphates. Treatment of Col-0 seedlings with methyl jasmonate (MeJA) caused a 2-fold increase in InsP$_8$, but only had subtle effects on other inositol polyphosphate species (as exemplified for various InsP$_5$ species; Figures 3C and 3D). A time-course experiment with MeJA-treated plants showed an almost 2-fold increase in levels of InsP$_8$ already after 15 min, which remained stable for the course of 3 h. In contrast, InsP$_7$ levels were not affected by MeJA treatment (Supplemental Figures 3C and 3D). Very different effects were observed in ABA-treated plants: ABA induced increases in both InsP$_7$ and InsP$_8$ in a dose-dependent manner (Supplemental Figure 3E).

To investigate the potential role of VIH2 in inositol pyrophosphate homeostasis, we analyzed two independent T-DNA insertion lines (*vih2-3* and *vih2-4*) that lack *VIH2* transcript (Supplemental Figures 4A and 4B). Overall incorporation of [^{3}H]-*myo*-inositol was not affected in these mutants (Supplemental

---

Figure 3. (continued).

shown. Asterisks indicate statistical differences (Student's *t* test; *P < 0.02). The isomeric identity of InsP$_{5b}$ is unknown in Arabidopsis seedlings. Based on chromatographic mobilities presented in a previous study on seedlings of Col-0 plants and *ipk1-1* plants (Stevenson-Paulik et al., 2005), and comparison with chromatographic mobilities of inositol polyphosphates in the same *ipk1-1* line on our HPLC (Supplemental Figures 8A and 8B), InsP$_{5a}$ represents Ins(1,3,4,5,6)P$_5$ and InsP$_{5c}$ represents Ins(1,2,4,5,6)P$_5$ or its enatiomer Ins(2,3,4,5,6)P$_5$.
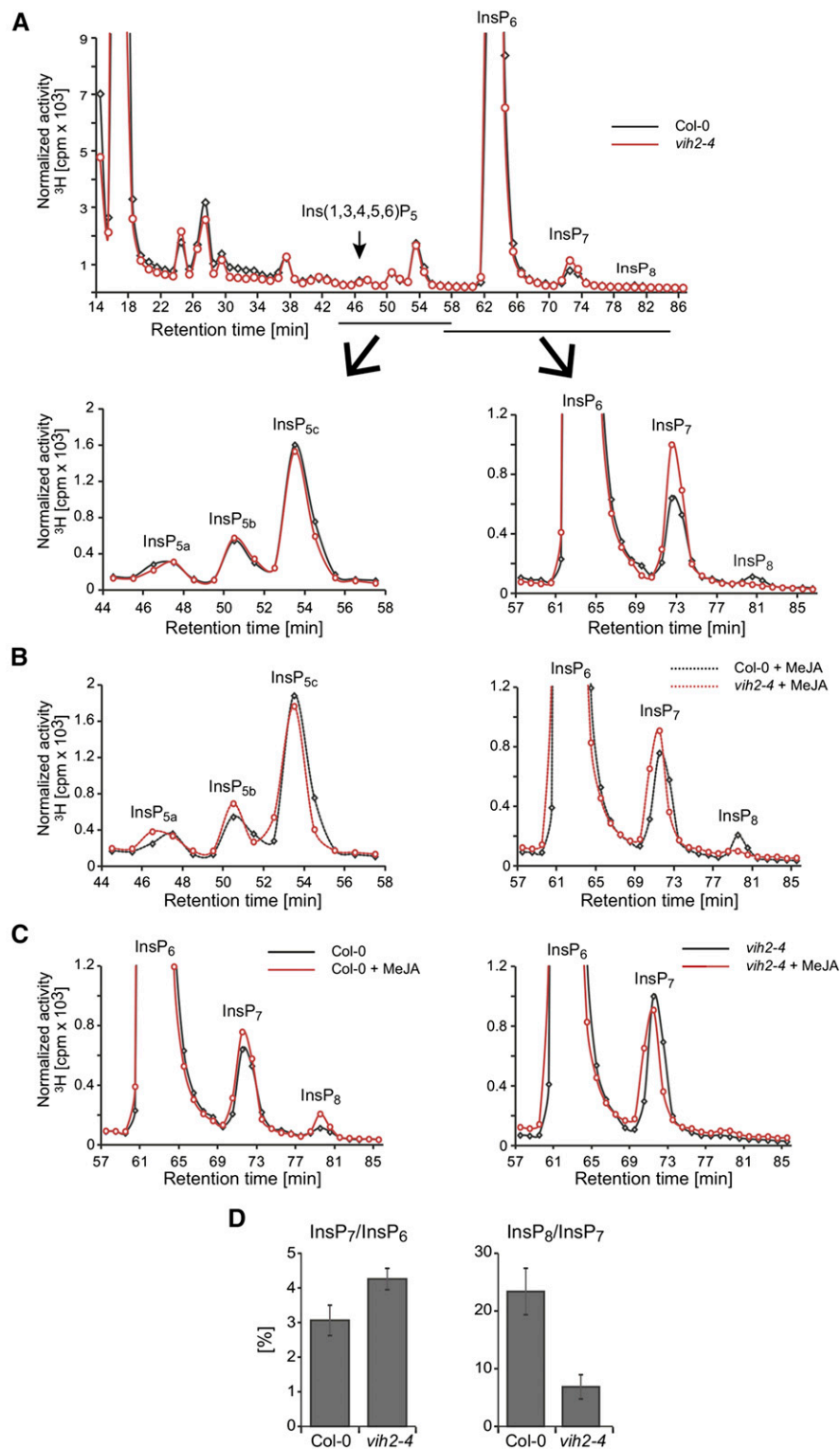
Figure 4. Bulk Steady State and Jasmonate-Induced Pools of InsP$_8$ in Arabidopsis Seedlings Depend on VIH2.

Normalized HPLC profiles (**[A]** to **[C]**) or relative amounts **(D)** of inositol phosphate species of 3-week-old [^{3}H] inositol-labeled Col-0 (solid black line) and *vih2-4* seedlings. In **(B)** and **(C)**, plants were treated with 50 µM MeJA and harvested after 30 min together with nontreated plants. Extracts were resolved by Partisphere SAX HPLC and fractions collected each minute for subsequent determination of radioactivity. The experiment was repeated

Figure 4C). HPLC profiles of *vih2* plants were similar to those of wild-type plants but showed a robust reduction of $InsP_8$ with a concomitant increase in $InsP_7$, suggesting that, like Vip1 in yeast, Arabidopsis VIH2 catalyzes the conversion of $InsP_7$ to $InsP_8$ (Figures 4A and 4D; Supplemental Figures 5A to 5C). Small residual levels of $InsP_8$ in *vih2* plants remained completely insensitive to MeJA, independent of the exposure time (30 min MeJA in Figures 4B and 4C; 4 h MeJA in Supplemental Figure 5D). In summary, these results show that in seedlings, $InsP_8$ levels are upregulated by MeJA treatment and that both bulk/steady state and MeJA-induced pools of $InsP_8$ depend on VIH2.

VIH2 Plays a Critical Role in Jasmonate-Regulated Defenses

We examined the functional role of VIH2 in the defense against Brassicaceae specialist *Pieris rapae* (small white butterfly) and the generalist *Mamestra brassicae* (cabbage moth) by monitoring larval development in a no-choice setup in which larvae are contained and allowed to only graze on one specific genotype. Both *P. rapae* and *M. brassicae* larvae feeding on *vih2* plants showed a significant weight increase compared with larvae feeding on Col-0 plants (Figures 5A and 5B), suggesting that VIH2 plays a role in activating defenses that interfere with insect herbivore development.

To examine whether decreased herbivore resistance was caused by compromised jasmonate production or perception, we analyzed jasmonates and jasmonate-responsive gene expression. To our surprise, upon mechanical wounding, *vih2* mutants exhibited increased levels of JA and bioactive conjugates such as JA-Leu/Ile and JA-Val compared with Col-0 (Figures 5C and 5D; Supplemental Figure 6A), an observation that is counterintuitive to decreased insect herbivore resistance in these plants. However, expression of *VSP2*, a marker gene of the MYC branch of JA signaling known to be induced by jasmonates and herbivores, was reduced in *vih2* plants after infestation with *P. rapae* larvae relative to Col-0 plants (Figure 5E; Supplemental Figure 6B). Similar results were obtained for *MYC2* expression (Figure 5E). These findings are in agreement with a reduced resistance of *vih2* plants in the performance assays. The observation that MYC-branch marker gene expression in *vih2* plants was reduced despite an increase in jasmonates suggests a defect in jasmonate perception. Supporting a defect in jasmonate-regulated defenses, *vih2* plants were also found to be more susceptible to the necrotrophic fungi *Botrytis cinerea* and *Alternaria brassicicola* (Supplemental Figures 6C and 6D).

Inositol Pyrophosphates Bind to the ASK1-COI1-JAZ Jasmonate Receptor Complex

To further investigate the role of VIH2 in jasmonate perception, we performed molecular docking of $Ins(1,2,4,5,6)P_5$, which

copurified with ASK1-COI1 from insect cells (Sheard et al., 2010), and $1,5-InsP_8$ into the proposed inositol polyphosphate binding pocket of the ASK1-COI1-JAZ1-JA-Ile complex. Poses with the highest scores (shown in Figures 6A and 6B) predict that the concave surface of the COI1 solenoid fold surrounds and binds molecules at overlapping, yet distinct, sites. An intricate network of basic COI1 residues (Lys-79, Lys-81, Arg-85, Arg-120, Arg-121, Arg-409, and Arg-440) and JAZ1 residue Arg-206 are predicted to coordinate $Ins(1,2,4,5,6)P_5$ and $1,5-InsP_8$ (Figures 6A and 6B). The $1,5-InsP_8$ molecule is predicted to be additionally stabilized by COI1 residues His-118, Arg-346, Tyr-382, and Lys-492, which coordinate the 1-β-phosphate, the 3-phosphate, the 3-phosphate, and the 5-β-phosphate of $1,5-InsP_8$, respectively. We investigated the involvement of three of these residues (His-118, Arg-346, and Lys-492; highlighted in Figure 6B) in COI1-JAZ1 interaction in a yeast two-hybrid system. These residues are positioned as an almost equilateral triangle (distance of respective coordinating groups: His-118, Lys-492, 13.01 Å; His-118-Arg-346, 13.06 Å; and Lys-492-Arg-346, 13.57 Å) and for geometrical reasons and assuming rigid ligand binding, not all three residues can interact with $Ins(1,2,4,5,6)P_5$ or other $InsP_5$ isomers (not containing diphosphobonds) simultaneously. Individual substitution of these amino acids (predicted to specifically coordinate $1,5-InsP_8$) by Ile completely abolished COI1-JAZ1 interaction, even though protein stability was not (His-118I and Lys-492I) or only mildly (Arg-346I) affected (Figures 6C and 6D). These results suggest a critical role of $InsP_8$ rather than $InsP_5$ isomers in COI1-JAZ1 complex formation.

To investigate whether inositol pyrophosphate can bind directly to the COI1-JAZ1 complex, we performed binding assays of ASK1-COI1-JAZ1 with radiolabeled $[^3H]$-$InsP_5$, $[^3H]$-$InsP_6$, and $[^3H]$-$InsP_7$ purified and desalted from $[^3H]$-*myo*-inositol-labeled seedlings as described in experimental procedures. Inositol polyphosphate binding was only observed in the presence of the structural JA-Ile analog coronatine, suggesting that inositol polyphosphates do not stimulate ASK1-COI1-JAZ1 complex formation in the absence of jasmonates (Figure 7A). Importantly, plant $InsP_7$ bound more efficiently than $InsP_6$, which bound more efficiently than $Ins(1,3,4,5,6)P_5$, indicating that inositol pyrophosphates are superior ligands of the ASK1-COI1-JAZ1 complex compared with less anionic inositol polyphosphate species (Figures 7A and 7B).

DISCUSSION

Inositol pyrophosphates have gained recent attention as signaling molecules in amoeba, yeast, and mammalian cells (Mulugu et al., 2007; Shears, 2009; Chakraborty et al., 2011; Szijgyarto et al., 2011; Wundenberg and Mayr, 2012; Pöhlmann et al., 2014). Here,

---

Figure 4. (continued).

with similar results, and representative results from one experiment are shown. **(B)** is a zoom-in into the $InsP_5$ (left) and $InsP_{6-8}$ (right) regions of HPLC runs with extracts of MeJA-treated Col-0 and *vih2* seedlings as indicated. For $InsP_{5a-c}$ isomer identities, see comment in Figure 3. **(C)** is a zoom-in into the $InsP_{6-8}$ regions of HPLC runs with extracts of Col-0 (left) and *vih2* (right) seedlings with or without MeJA treatment as indicated. For relative amounts **(D)**, data are presented either as $InsP_7/InsP_6$ ratio (a measure of IP6K activity) or as $InsP_8/InsP_7$ ratio (a measure of PPIP5K activity). The data represent means ± SE.
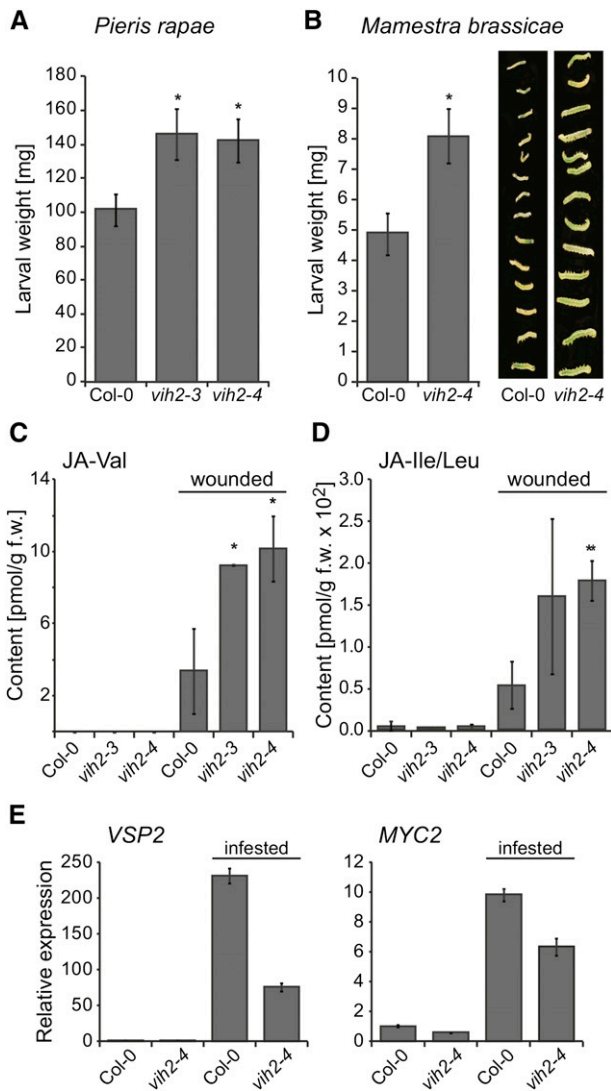
Figure 5. Arabidopsis *vih2* Lines Have Reduced Defenses against Larvae of Herbivorous Insects and Are Compromised in Jasmonate Perception.

(A) and **(B)** Larval development was monitored in a no choice setup. One caterpillar each (larval stage L1) of the Brassicaceae specialist *P. rapae* **(A)** or the generalist *M. brassicae* **(B)** was released onto a single 5-week-old plant (*n* = 20) of the designated genotype. Fresh weight of caterpillars was determined after 7 d (*P. rapae*) or 8 d (*M. brassicae*). The values represent means ± SE. Asterisks indicate statistical differences (Student's *t* test; *P < 0.02). Plant genotype-dependent size differences of *M. brassicae* larvae are also visualized by a photograph (**[B]**, right panel). Experiments were repeated with similar results.
(C) and **(D)** Determination of bioactive conjugates JA-Val and JA-Ile/Leu. Conjugate levels were determined in rosette leaves of 4-week-old plants of designated genotypes under sterile conditions and 3 h after inflicting wounding by squeezing each leaf with forceps. Data represent means of three independent biological replica ± SD. Statistical significance is indicated by asterisks (Student's *t* test; *P < 0.02 and **P < 0.005).
(E) qPCR analysis of JA-dependent genes. Gene expression was analyzed by qPCR analyses using RNA extracted from pooled leaves (*n* = 5)

we describe the presence of $InsP_7$ and $InsP_8$ in the model plant Arabidopsis and show that VIH2 is a functional inositol pyrophosphate synthetase responsible for $InsP_8$ production, playing a critical role in jasmonate-regulated defenses. The ubiquitous presence of Vip1/PPIP5K homologs in plants as suggested by our work supports and extends previous reports of the wide distribution of these enzymes in eukaryotic organisms and underlines the fundamental importance of inositol pyrophosphates in regulating cellular functions.

VIH Proteins Have Vip1/PPIP5K-Like Activities

A structural model of the VIH2 ATP-grasp kinase domain and complementation of defects in growth and inositol polyphosphate homeostasis of yeast *vip1* mutants indicate that VIH1 and VIH2 execute Vip1/PPIP5K-like activities and are likely to pyrophosphorylate the 1-position of $InsP_6$ and 5-$InsP_7$ in yeast (Figure 2). A recent study by Desai et al. (2014) that was published while this article was in preparation also addressed the function of Arabidopsis Vip1 homologs. Similar to the experiment shown in Figure 2E, the authors show that expression of these proteins in a yeast *vip1Δ kcs1Δ ddp1Δ* triple mutant results in $InsP_7$ production. Based on these results, the authors predicted a role of these enzymes as IP6K ($InsP_6$ kinase) enzymes. Unfortunately, this experiment does not allow discrimination between Kcs1/IP6K and Vip1/PPIP5K activities because Vip1/PPIP5K enzymes are well known to efficiently use $InsP_6$ as a substrate to produce (1-)$InsP_7$ (Mulugu et al., 2007; Lin et al., 2009; Losito et al., 2009). We therefore investigated the ability of VIH proteins to complement single mutant *kcs1Δ* or *vip1Δ* yeast phenotypes and analyzed the role of VIH2 in planta. We show that VIH proteins rescue *vip1Δ*-associated growth defects on 6-azauracil, whereas they fail to rescue *kcs1Δ*-associated growth defects (Figures 2C, 2D, and 2G). Furthermore, we show that VIH2 complements the *vip1Δ*-associated defect in $InsP_7$ to $InsP_8$ conversion (Figure 2F; Supplemental Figure 2C) and that *vih2* lines are compromised in $InsP_8$ synthesis and (similar to yeast *vip1Δ* mutants) accumulate $InsP_7$ (Figures 4B and 4D; Supplemental Figure 5). Collectively, these data provide strong evidence that in vivo VIH proteins do not execute IP6K/Kcs1-like activities as suggested by Desai et al. (2014) but PPIP5K/Vip1-like activities.

The Isomer Identity of Plant Inositol Pyrophosphates Remains Unresolved

The expression pattern of *VIH2* and the pronounced effect on seedling $InsP_8$ production observable in *vih2* plants indicate that VIH2 is the major enzyme synthesizing $InsP_8$ in Arabidopsis (Figures 3 and 4; Supplemental Figures 5A and 5B). It remains unclear, however, whether plant $InsP_7$ and $InsP_8$ have the same isomer identity as in yeast. Anion exchange HPLC

of 5-week-old plants of the designated genotype that were untreated or infested for 24 h by *P. rapae* larvae as indicated. *PP2AA3* was used as a reference gene. The expression value of untreated Col-0 was set to 1. Shown are means ± SE (*n* = 3). qPCR analyses were repeated with similar results.
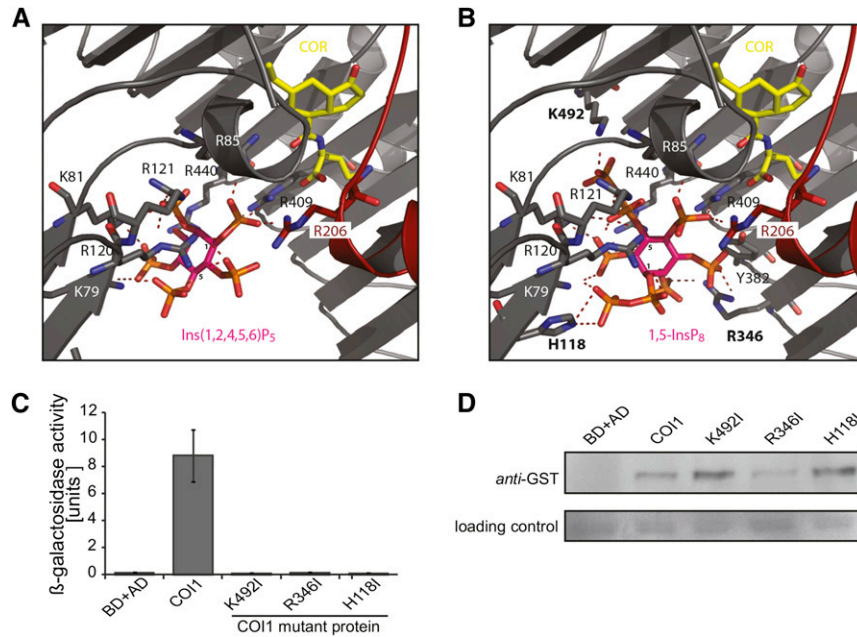
Figure 6. Structural Models of ASK1-COI1-JAZ1-Coronatine in Complex with Ins(1,2,4,5,6)P$_5$ or 1,5-InsP$_8$ and Functional Evaluation of Proposed 1,5-InsP$_8$ Binding Mutants Suggest a Role of InsP$_8$ in Jasmonate Receptor Complex Formation.

(A) and **(B)** COI1-JAZ structures containing Ins(1,2,4,5,6)P$_5$ or 1,5-InsP$_8$ as obtained from in silico docking experiments are shown. COI1 (gray ribbon), coronatine (COR) in yellow stick representation, and inositol polyphosphates (rendered as stick in magenta) are presented. Hydrogen bonds and salt bridge networks are depicted as dashed lines. Residues in bold were substituted by Ile for yeast two-hybrid studies.

(C) JAZ1 interaction with wild-type or mutant COI1 in yeast was evaluated in the presence of 50 μM coronatine by coexpression of pGBKT7-*COI1* (and mutated versions as indicated) with pGADT7-*JAZ1* in yeast strain Y187 (Clontech) and subsequent quantification of β-galactosidase-mediated hydrolysis of ortho-nitrophenyl-β-D-galactopyranoside. Values represent means of four independent biological replica ± SD.

(D) Stability of mutant COI1 protein. Immunoblots of soluble lysates prepared from tobacco (*Nicotiana benthamiana*) leaves expressing COI1 mutants (as designated) in translational fusion with N-terminal GST. Equal amounts of total protein were loaded, and COI1 was detected with antibodies against GST (Sigma-Aldrich). As a normalization control (lower panel), a representative unspecific band was chosen.

chromatography does not allow unambiguous discrimination between different inositol pyrophosphate isomers of same molecular mass. Two major observations challenge the idea that yeast and plant InsP$_7$ and InsP$_8$ isomers are identical. First, BLAST search analyses did not allow the identification of plant Kcs1/IP6K homologs, suggesting that an unknown enzyme

activity is responsible for plant InsP$_7$ production. Second, plant-purified InsP$_7$ exhibits a higher binding affinity for the ASK1-COI1-JAZ1 jasmonate receptor complex than InsP$_6$ or InsP(1,3,4,5,6)P$_5$ (Figure 7B). In contrast, competition assays following a similar strategy recently employed to evaluate InsP$_7$ binding to human casein kinase-2 (Rao et al., 2014) showed that available
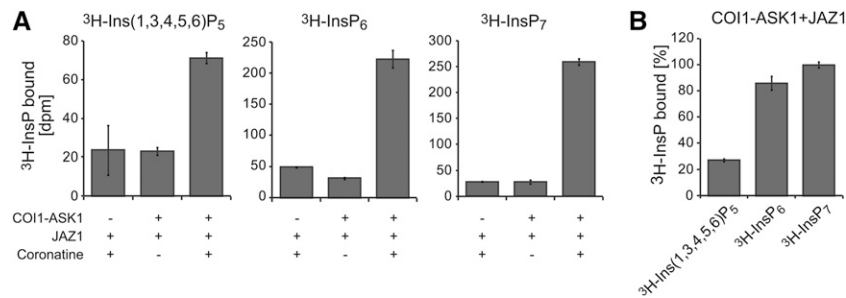
Figure 7. Plant Inositol Pyrophosphates Are Superior Ligands of the ASK1-COI1-JAZ1 Complex Compared with Less Anionic Inositol Polyphosphate Species.

Direct binding of [^{3}H]-InsP$_5$, [^{3}H]-InsP$_6$, and [^{3}H]-InsP$_7$ (purified and desalted from [^{3}H]-*myo*-inositol labeled seedlings of the *ipk1-1* mutant [InsP$_5$] or Col-0 seedlings [InsP$_6$ and InsP$_7$]) to the ASK1/COI1/His$_8$-MBP-JAZ1 jasmonate receptor complex or to individual components of the receptor complex (ASK1-COI1 or His$_8$-MBP-JAZ1) was analyzed with or without 1 μM coronatine. A total activity of 2000 dpm was used for each [^{3}H]-labeled inositol phosphate species. The average of recovered radiolabel with [^{3}H]-InsP$_7$ in **(B)** is set to 100%. Values show means ± SE (*n* = 2 or 3) of radiolabel recovered by pull-down of His$_8$-MBP-JAZ1 via metal affinity chromatography, and experiments were repeated with similar results.
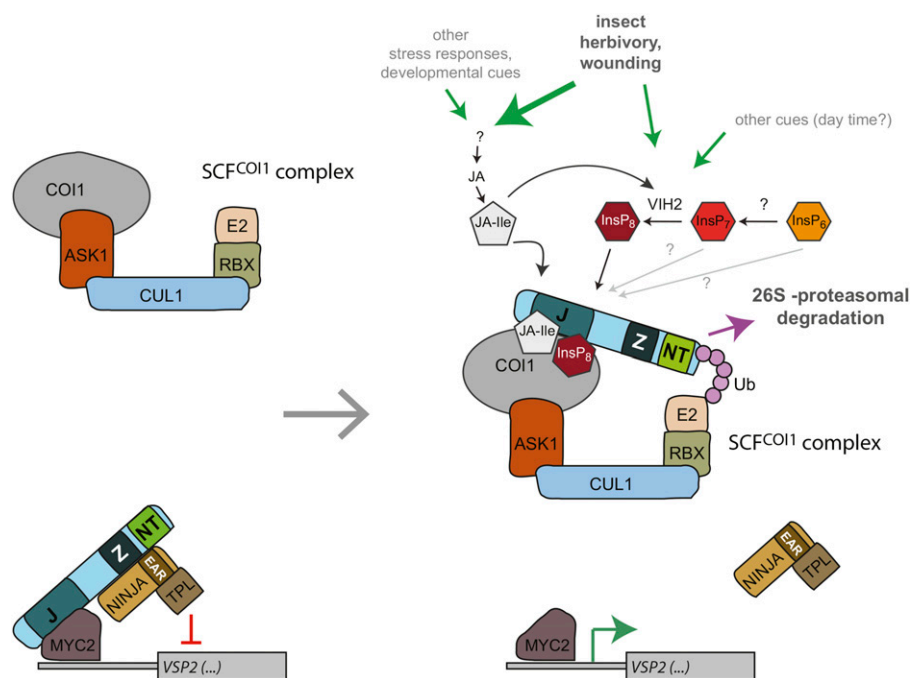
Figure 8. Model of the Role of VIH2 and InsP$_8$ in the Wound Response.

Mechanical wounding or herbivore attack stimulate the synthesis of JA and bioactive JA conjugates such as JA-Ile. Increasing jasmonate levels trigger a fast VIH2-dependent increase in InsP$_8$, which is most likely caused by posttranslational activation of the VIH2 protein. Both JA-Ile and InsP$_8$ occupy designated binding pockets in COI1-ASK1 and might work as molecular glue to recruit the JAZ repressor protein. Subsequent polyubiquitylation of JAZ by the SCF ubiquitin E3 ligase complex causes proteasomal degradation of the JAZ repressor and allows expression of jasmonate/InsP$_8$-responsive genes such as *VSP2*. The physiological role of other inositol polyphosphates on potentiating jasmonate dependent formation of the SCF^{COI1} ubiquitin E3 ligase complex remains unclear.

chemically synthesized InsP$_7$ isomers have lower affinities than InsP$_6$ (1-InsP$_7$, 5-InsP$_7$, and 6-InsP$_7$) or a similar affinity (4-InsP$_7$) for the jasmonate receptor complex (Supplemental Figures 7A to 7C). Future research will have to address purification of plant InsP$_7$ in sufficient amounts for NMR analyses or crystallography to reveal plant InsP$_7$ (and by extension InsP$_8$) isomer identity. Equally important for future studies will be the identification of the protein(s) responsible for plant InsP$_7$ synthesis.

Plant InsP$_8$ Has a Role in Resistance against Insect Herbivores and Necrotrophic Fungal Pathogens

The finding that ABA induces InsP$_7$ and InsP$_8$ production (Supplemental Figure 3E), whereas MeJA induces production of primarily InsP$_8$ and not InsP$_7$ (Figures 3C, 3D, and 4C; Supplemental Figures 3C and 3D) identifies interesting interactions between jasmonate and ABA signaling that are distinct from those reported previously (Pieterse et al., 2012). Several lines of evidence suggest that plant InsP$_8$ is responsible for the VIH2-dependent contribution to resistance against herbivores and necrotrophs: (1) *vih2*-mutant seedlings have robustly decreased levels of InsP$_8$ and exhibit a decreased resistance against larvae of herbivorous insects and necrotrophs and have a defect in jasmonate perception (Figures 4 and 5; Supplemental Figures 5 and 6); (2) MeJA treatment causes a robust and specific increase in a VIH2-dependent pool of InsP$_8$ (Figures 3 and 4;

Supplemental Figures 3 and 5); (3) direct binding assays suggest that plant-derived inositol pyrophosphate (InsP$_7$) binds more efficiently to the ASK1-COI1-JAZ1 complex than less anionic inositol polyphosphates such as InsP$_6$ and Ins(1,3,4,5,6)P$_5$ (Figure 7B); (4) the proposed inositol polyphosphate binding pocket of the ASK1-COI1-JAZ1 jasmonate receptor complex is large enough to accommodate a single InsP$_8$ molecule (Figures 6A and 6B) and COI1 mutants designed to specifically prevent InsP$_8$ binding failed to interact with JAZ1 in yeast (Figure 6C). Unfortunately, we failed to purify sufficient amounts of plant derived InsP$_8$ to perform radioligand binding based reconstitution assays, which will be an important task for future work.

Our study does not rule out that other inositol polyphosphates may influence assembly of the jasmonate receptor complex. Ins(1,2,4,5,6)P$_5$, which copurified with the ASK1-COI1 complex from insect cells (Sheard et al., 2010), is an interesting candidate in this regard. However, it is unclear whether plants synthesize Ins(1,2,4,5,6)P$_5$ or its enantiomer Ins(2,3,4,5,6)P$_5$ (Stevenson-Paulik et al., 2005; Hanke et al., 2012), and a physiological significance of either species in herbivore resistance has not been established so far. Another isomer, Ins(1,3,4,5,6)P$_5$, that highly accumulates in *ipk1-1* plants (Supplemental Figure 8) has been implicated in the increased herbivore resistance of this plant mutant (Mosblech et al., 2011). While it remains to be shown whether this InsP$_5$ isomer has any function in ASK1-COI1-JAZ complex formation in the context of a wild-type plant, we can

exclude the possibility that it plays a role in VIH2-dependent insect herbivore resistance because Ins(1,3,4,5,6)P$_5$ levels did not change in *vih2* lines (Figures 4A and 4B; Supplemental Figures 5A and 5B).

Coincidence Detection of Jasmonate and Inositol Phosphates by the Jasmonate Coreceptor

Direct binding assays with [^{3}H]-Ins(1,3,4,5,6)P$_5$, [^{3}H]-InsP$_6$, and [^{3}H]-InsP$_7$ (Figures 7A and 7B) indicate that inositol polyphosphate binding is not sufficient for ASK1-COI1-JAZ1 assembly but still requires the presence of coronatine (or by extension JA-Ile). Combined with the previous observation that coronatine fails to trigger the formation of the ASK1-COI1-JAZ complex in the absence of inositol polyphosphate (Sheard et al., 2010), these data suggest that only coincidence detection of both inositol polyphosphate or pyrophosphate and bioactive jasmonate allows complex formation and subsequent proteasomal degradation of JAZ repressor proteins to stimulate jasmonate responsive gene expression (Figure 8). We propose that coincidence detection of two unrelated molecules might prevent an uncontrolled accidental trigger of immune responses that are known to severely affect plant growth and development (Pieterse and Dicke, 2007; Howe and Jander, 2008). This idea is in agreement with a recent finding that COI1 protein levels are strictly regulated by a dynamic balance between SCF^{COI1}-mediated stabilization and 26S proteasome-mediated degradation (Yan et al., 2013).

In addition, coincidence detection could allow differentiated immune responses. It still remains a central unanswered question how plants achieve specificity in their response to herbivore attack. It has been shown, for instance, that transcriptional responses of Arabidopsis to caterpillar (*P. rapae*) and thrips (*Frankliniella occidentalis*) infestation is primarily via COI1-dependent gene regulation, but that expression patterns of these genes are specific to one or the other insect herbivore (De Vos et al., 2005). We speculate that a differentiation in COI1-dependent responses might be in part determined by the inositol pyrophosphate signature of a given tissue under herbivore attack. It is important to note that InsP$_6$ also has previously been suggested to play an important role in the maintenance of basal resistance to plant pathogens. The reduction of InsP$_6$ in potato and Arabidopsis was correlated with increased susceptibility toward different viral infections and also caused hypersensitivity to fungal and bacterial infections in Arabidopsis (Murphy et al., 2008). In future experiments, it will be important to study whether these effects are an immediate consequence of reduced InsP$_6$ or whether they are caused by the reduction of InsP$_6$-dependent inositol pyrophosphates. Independent of this outcome, breeding strategies and biotechnological approaches to reduce InsP$_6$ will have to consider possible negative side effects in crop plants.

METHODS

BLAST Search and Phylogenetic Analyses

Sequence sampling focused on plants and fungi with some additions of protist species. BLAST search analyses (http://blast.ncbi.nlm.nih.gov/ Blast.cgi) were performed using the N-terminal part of *Saccharomyces cerevisiae* Vip1 (residues 1 to 535), which contains the entire ATP-grasp kinase domain (Mulugu et al., 2007). The amino acid sequences were aligned using MAFFT, version 6.927b (Katoh et al., 2005). Heterogeneous alignment regions were excluded prior to phylogenetic analyses using Gblocks (Castresana, 2000), with the minimum length of a block set to five, allowing gaps in up to 50% of the sequences at a given site, a minimum number of sequences of 24 for a conserved or a flanking position, and a maximum number of contiguous nonconserved positions of eight. A phylogenetic tree was estimated using maximum likelihood (Felsenstein, 1981) with RAxML version 7.3.2 (Stamatakis, 2006a). Fast bootstrap analyses (Felsenstein, 1985; Stamatakis et al., 2008) over 10,000 rounds were run on the Web-based bioportal facility (Kumar et al., 2009) (http://www.mn.uio.no/ibv/bioportal/) with eight parallel processors, using bootstrap trees as starting trees for heuristic searches, and employing the DAYHOFF model of amino acid substitution as inferred with the ProteinModelSelection perl script (http://www.exelixis-lab.org/), accounting for rate heterogeneity by using the CAT model (Stamatakis, 2006b). The final tree was optimized using the Gamma model of rate heterogeneity (Yang, 1993).

Plants and Growth Conditions

For T-DNA insertion lines, seeds of mutant lines of *Arabidopsis thaliana* (ecotype Col-0) were obtained from The European Arabidopsis Stock Centre (http://arabidopsis.info/). The T-DNA lines used in this study are as follows: *vih2-3a* (SAIL_165_F12), *vih2-4* (GK-080A07), and *ipk1-1* (SALK_065337C). Homozygous lines were identified by PCR using T-DNA left and right border primers and gene-specific sense or antisense primers (Supplemental Table 1). The isolated homozygous progeny of the *vih2-3a* line identified by PCR-based genotyping was found to have short root hairs compared with Col-0. However, the phenotype did not cosegregate with the *vih2-3* allele in the F2 generation of a cross with the *vih1-1* T-DNA line (SAIL_543_F08), suggesting that the original *vih2-3a* plant had an additional insertion or mutation causing the root hair phenotype. Therefore, *vih2-3a* was crossed with a *VIH2* wild-type plant (Col-0 background) and F3 progeny homozygous for the *vih2-3* allele (exhibiting normal root hairs) used for further analyses. All lines analyzed in this study, including Col-0 plants, were grown in parallel for two generations under identical conditions on soil (16 h light and 8 h dark, day/night temperature 22/18°C and 120 μmol^{-1} m^{-2} light intensity), and seeds of the respective last progenies were used for all analyses described in this article. For growth in sterile conditions, seeds were sterilized in 70% (v/v) ethanol and 0.05% (v/v) Triton X-100 for 30 min and washed twice in 90% (v/v) ethanol. Sterilized seeds were plated onto 0.5× MS, 1% sucrose, 0.7 to 0.8% phytagel stratified for 2 d at 4°C, and grown under conditions of 12 h light (23°C) and 12 h dark (21°C). To investigate the expression of distinct *VIH2* domains in the respective T-DNA insertion lines, qPCR analyses were performed using the primers listed in Supplemental Table 2.

Performance and Disease Assays

Plants were grown at standard growth conditions in the greenhouse as described earlier (Verhage et al., 2011). Freshly hatched larvae (L1 stage) of the Brassicaceae specialist *Pieris rapae* (small cabbage white butterfly) or the generalist *Mamestra brassicae* (cabbage moth) were released onto fully expanded rosette leaves of 5-week-old plants of the designated genotype. Individual plants of the designated genotype were infested with a single caterpillar of either *P. rapae* or *M. brassicae*. The caterpillar-challenged plants were placed in a transparent plastic container sealed with insect-proof meshes allowing adequate gas exchange and light transmission. Fresh weight of caterpillars was measured after 7 d (*P. rapae*) or 8 d (*M. brassicae*) of feeding.

Botrytis cinerea and *Alternaria brassicicola* assays were performed as previously described (Kemmerling et al., 2007; Van Wees et al., 2013).

Chemicals

Coronatine, methyl jasmonate, and abscisic acid were from Sigma-Aldrich. 2-Nitrophenyl-β-D-galactopyranoside was from Applichem. $InsP_6$ was from Sichem. 1-$InsP_7$, 4-$InsP_7$, 5-$InsP_7$, 6-$InsP_7$, and 1,5-$InsP_8$ were synthesized as recently described (Capolicchio et al., 2013, 2014). [^{3}H]-$InsP_6$ and [^{3}H]-$InsP_7$ were extracted and purified from [^{3}H]-*myo*-inositol-labeled Col-0 seedlings using a desalting protocol as described earlier (Azevedo et al., 2010). [^{3}H]-Ins(1,3,4,5,6)P_5 was purified from [^{3}H]-*myo*-inositol-labeled *ipk1-1* seedlings using the same desalting protocol. Standards were [^{3}H]-$InsP_6$ (Azevedo and Saiardi, 2006) and [^{3}H]-5-$InsP_7$ that was generated in vitro from [^{3}H]-$InsP_6$ and recombinant mammalian IP6K1 (Azevedo et al., 2010).

In Vitro Binding Assays

In vitro binding assays were performed with recombinant COI1-ASK1 and His$_8$-MBP-JAZ in 1:2 molar ratios. Purified and desalted [^{3}H]-$InsP_6$ was added to the reaction buffer containing 50 mM Tris-HCl, pH 7.5, 100 mM NaCl, 10 mM imidazole, 10% (v/v) glycerol, 0.1% (v/v) Tween 20, and 5 mM 2-mercaptoethanol in a total volume of 0.5 mL. Unless mentioned otherwise, [^{3}H]-$InsP_6$ at a total activity of 4000 dpm and 1 μM coronatine was added to each reaction. The reaction was incubated at room temperature (22 to 24°C) for 90 min, then 30 μL of Ni-NTA resin was added with a further incubation at 4°C for 90 min. The resin was centrifuged for 5 min at 900*g* and washed three times with ice-cold reaction buffer. Proteins were eluted with 250 mM imidazole and recovered radioactivity analyzed by scintillation counting.

Extraction and HPLC Analyses of Inositol Phosphates

Inositol polyphosphates from yeast were extracted and analyzed as described (Azevedo and Saiardi, 2006). Extraction and measurement of inositol polyphosphates from Arabidopsis seedling were performed as follows. Seedlings were grown under sterile conditions in liquid 0.5× MS with 2% sucrose for 10 d and then transferred to sucrose-free low MS semi-liquid medium (0.25 MS and 0.3% Phytagel). Labeling was started at 2 weeks of age by addition of 40 μCi mL^{-1} of [^{3}H]-*myo*-inositol (30 to 80 Ci mmol^{-1} and 1 mCi mL^{-1}; Biotrend; ART-0261-5) for 2 mL liquid MS media containing 10 seedlings. After 6 d of labeling, leaves or seedlings were washed two times with ultrapure water before harvesting and freezing into liquid N_2. Inositol polyphosphates were extracted as described previously (Azevedo and Saiardi, 2006) and resolved by strong anion exchange chromatography HPLC (using the partisphere SAX 4.6 × 125 mm column; Whatman) at a flow rate of 0.5 mL min^{-1} with the gradient of buffers A (1 mM EDTA) and B [1 mM EDTA and 1.3 M $(NH_4)_2HPO_4$, pH 3.8, with H_3PO_4] following the standard protocol mentioned above. Fractions were collected each minute, mixed with scintillation cocktail (Perkin-Elmer; ULTIMA-FLO AP), and analyzed by scintillation counting. To account for differences in fresh weight and extraction efficiencies between samples, values shown are normalized activities based on the total activity of each sample. To avoid misleading results derived from unincorporated [^{3}H]-*myo*-inositol in the HPLC run, "total" activities for normalization were calculated by counting fractions from 17 min (Figures 2F and 2G; Supplemental Figures 2C and 2D), 22 min (Figure 3C; Supplemental Figures 2E, 3B, and 5A), or from 18 min (Figure 4) until the end of runs. HPLC runs within an experimental set were normalized in the following way: If sample B had less "total" activity than sample A, the equation used for normalization was −[individual data point of sample A*("total" InsP of B/"total" InsP of A)]. Results are presented as minute fractions (circle or diamond) connected by lines.

Total RNA Extraction and qPCR Analyses

Leaf samples (up to 100 mg) were harvested for total RNA extraction using the RNeasy Plant Mini Kit (Qiagen). A total of 1 μg RNA was used for cDNA preparation following DNaseI digest (Fermentas). The reverse transcription was done according to the manufacturer's instructions (Roboklon; AMV Reverse Transcriptase Native). The qPCR was performed with the SYBR Green reaction mix (Bioline; Sensimix SYBR No-ROX kit) in a Bio-Rad CFX384 real-time system. Data were analyzed using the Bio-Rad CFX Manager 2.0 (admin) system. *PP2AA3* or β-*TUBULIN* was used as a reference gene.

Yeast Two-Hybrid Assays

The full-length coding sequences of *COI1* and *JAZ1* were cloned into the yeast two-hybrid vector pGBKT7 and pGADT7, respectively, in fusion with N-terminal binding domain or activation domain. The yeast strain Y187 was transformed with individual wild-type or *COI1* mutant constructs generated by site-directed mutagenesis (see above) together with *JAZ1* construct following the standard yeast transformation protocol mentioned above. Yeast transformants were selected on solid CSM-Leu-Trp media after which single fresh colonies from independent transformants were grown overnight in liquid CSM-Leu-Trp media. JAZ1 interaction with wild-type or mutant COI1 in the presence of 50 μM coronatine was evaluated by quantification of β-galactosidase-mediated hydrolysis of ortho-nitrophenyl-β-D-galactopyranoside.

Accession Numbers

Sequence data from this article can be found in the Arabidopsis Genome Initiative or GenBank/EMBL databases under the following accession numbers: *VIH1* (At5g15070), *VIH2* (At3g01310), *MYC2* (At1g32640), *VSP2* (At5g24770), *PP2AA3* (AT1G13320), β-*TUBULIN* (AT5G62700), *JAZ1* (At1g19180), *COI1* (At2g39940), *IPK1* (At5g42810), *Saccharomyces cerevisiae VIP1* (YLR410W), *S. cerevisiae KCS1* (YDR017C), and *hPPIP5K2* (NM_001276277). Accession numbers for T-DNA insertion lines are as follows: *vih2-3a* (SAIL_165_F12), *vih2-4* (GK-080A07), *ipk1-1* (SALK_065337C), and *vih1-1* T-DNA line (SAIL_543_F08).

Supplemental Data

Supplemental Figure 1. Two-domain Architecture, Structural Conservation of the ATP-Grasp Domain, and Conserved Binding Residues Suggest That VIH Proteins Are Functional PPIP5 Kinases.

Supplemental Figure 2. VIH Proteins Are Functional Inositol Pyrophosphate Synthetases in Yeast.

Supplemental Figure 3. A Time-Course Experiment Reveals a Fast and Specific Induction of $InsP_8$ by MeJA.

Supplemental Figure 4. Genome Structure and Identification of *vih2*::T-DNA Insertion Lines.

Supplemental Figure 5. Bulk Steady State and Jasmonate-Induced Pools of $InsP_8$ in Arabidopsis Seedlings Depend on VIH2.

Supplemental Figure 6. VIH2 Regulates Jasmonate Perception.

Supplemental Figure 7. Different Inositol Polyphosphates Exhibit Distinct Binding Affinities for the ASK1-COI1-JAZ Jasmonate Receptor Complex.

Supplemental Figure 8. Detection of Inositol Pyrophosphate in the *ipk1-1* Mutant Line.

Supplemental Table 1. Primer List for PCR-Based Characterization of T-DNA Insertion Lines.

Supplemental Table 2. Primer List for qPCR Analyses.

Supplemental Table 3. Primer List for Generation of pDR195-Based Yeast Episomal Expression Vectors.

Supplemental Table 4. List of Primer Sequences Used for Site-Directed Mutagenesis.

Supplemental Table 5. Primers and Plasmids Used to Generate Yeast Knockout Strains.

Supplemental Table 6. Primers Used to Clone *JAZ* Homolog into the pET28- His$_8$-MBP Bacterial Expression Vector

Supplemental Methods.

Supplemental References.

Supplemental Data Set 1. Text File of the Sequences and Alignment Used for the Phylogenetic Analysis Shown in Figure 1.

AUTHOR CONTRIBUTIONS

D.L., S.C.M.V.W., A.S., and G.S. designed the research. D.L., P.J., C.A., M.D., S.C., H.M., T.I., M.S., M.F., P.G., M.F.K.D.C, A.S., and G.S. performed the experiments. D.L., P.J., C.A., M.D., M.W., N.Z., I.F., H.J.J., S.C.M.V.W., A.S., and G.S. analyzed the data and revised the article. D.L. and G.S. wrote the article.

REFERENCES

Azevedo, C., and Saiardi, A. (2006). Extraction and analysis of soluble inositol polyphosphates from yeast. Nat. Protoc. **1:** 2416–2422.

Azevedo, C., Burton, A., Ruiz-Mateos, E., Marsh, M., and Saiardi, A. (2009). Inositol pyrophosphate mediated pyrophosphorylation of AP3B1 regulates HIV-1 Gag release. Proc. Natl. Acad. Sci. USA **106:** 21161–21166.

Azevedo, C., Burton, A., Bennett, M., Onnebo, S.M., and Saiardi, A. (2010). Synthesis of InsP7 by the Inositol Hexakisphosphate Kinase 1 (IP6K1). Methods Mol. Biol. **645:** 73–85.

Barker, C.J., Illies, C., Gaboardi, G.C., and Berggren, P.O. (2009). Inositol pyrophosphates: structure, enzymology and function. Cell. Mol. Life Sci. **66:** 3851–3871.

Blackwell, M., Vilgalys, R., James, T.Y., and Taylor, J.W. (2012). Fungi. Eumycota: mushrooms, sac fungi, yeast, molds, rusts, smuts, etc. In The Tree of Life Web Project, http://tolweb.org/.

Blatt, M.R., Thiel, G., and Trentham, D.R. (1990). Reversible inactivation of K$^+$ channels of Vicia stomatal guard cells following the photolysis of caged inositol 1,4,5-trisphosphate. Nature **346:** 766–769.

Brearley, C.A., and Hanke, D.E. (1996). Inositol phosphates in barley (*Hordeum vulgare* L.) aleurone tissue are stereochemically similar to the products of breakdown of InsP6 in vitro by wheat-bran phytase. Biochem. J. **318:** 279–286.

Burnette, R.N., Gunesekera, B.M., and Gillaspy, G.E. (2003). An Arabidopsis inositol 5-phosphatase gain-of-function alters abscisic acid signaling. Plant Physiol. **132:** 1011–1019.

Burton, A., Hu, X., and Saiardi, A. (2009). Are inositol pyrophosphates signalling molecules? J. Cell. Physiol. **220:** 8–15.

Capolicchio, S., Thakor, D.T., Linden, A., and Jessen, H.J. (2013). Synthesis of unsymmetric diphospho-inositol polyphosphates. Angew. Chem. Int. Ed. Engl. **52:** 6912–6916.

Capolicchio, S., Wang, H., Thakor, D.T., Shears, S.B., and Jessen, H.J. (2014). Synthesis of densely phosphorylated bis-1,5-diphospho-myo-inositol tetrakisphosphate and its enantiomer by bidirectional P-anhydride formation. Angew. Chem. Int. Ed. Engl. **53:** 9508–9511.

Castresana, J. (2000). Selection of conserved blocks from multiple alignments for their use in phylogenetic analysis. Mol. Biol. Evol. **17:** 540–552.

Chakraborty, A., Kim, S., and Snyder, S.H. (2011). Inositol pyrophosphates as mammalian cell signals. Sci. Signal. **4:** re1.

Chen, X., Lin, W.H., Wang, Y., Luan, S., and Xue, H.W. (2008). An inositol polyphosphate 5-phosphatase functions in PHOTOTROPIN1 signaling in Arabidopsis by altering cytosolic Ca^{2+}. Plant Cell **20:** 353–366.

Chini, A., Fonseca, S., Fernández, G., Adie, B., Chico, J.M., Lorenzo, O., García-Casado, G., López-Vidriero, I., Lozano, F.M., Ponce, M.R., Micol, J.L., and Solano, R. (2007). The JAZ family of repressors is the missing link in jasmonate signalling. Nature **448:** 666–671.

De Vos, M., Van Oosten, V.R., Van Poecke, R.M., Van Pelt, J.A., Pozo, M.J., Mueller, M.J., Buchala, A.J., Métraux, J.P., Van Loon, L.C., Dicke, M., and Pieterse, C.M. (2005). Signal signature and transcriptome changes of Arabidopsis during pathogen and insect attack. Mol. Plant Microbe Interact. **18:** 923–937.

Desai, M., Rangarajan, P., Donahue, J.L., Williams, S.P., Land, E.S., Mandal, M.K., Phillippy, B.Q., Perera, I.Y., Raboy, V., and Gillaspy, G.E. (2014). Two inositol hexakisphosphate kinases drive inositol pyrophosphate synthesis in plants. Plant J. **80:** 642–653.

Dorsch, J.A., Cook, A., Young, K.A., Anderson, J.M., Bauman, A.T., Volkmann, C.J., Murthy, P.P., and Raboy, V. (2003). Seed phosphorus and inositol phosphate phenotype of barley low phytic acid genotypes. Phytochemistry **62:** 691–706.

Draskovic, P., Saiardi, A., Bhandari, R., Burton, A., Ilc, G., Kovacevic, M., Snyder, S.H., and Podobnik, M. (2008). Inositol hexakisphosphate kinase products contain diphosphate and triphosphate groups. Chem. Biol. **15:** 274–286.

Felsenstein, J. (1981). Evolutionary trees from DNA sequences: a maximum likelihood approach. J. Mol. Evol. **17:** 368–376.

Felsenstein, J. (1985). Confidence limits on phylogenies: an approach using the bootstrap. Evolution **39:** 783–791.

Flores, S., and Smart, C.C. (2000). Abscisic acid-induced changes in inositol metabolism in *Spirodela polyrrhiza*. Planta **211:** 823–832.

Gillaspy, G.E. (2013). The role of phosphoinositides and inositol phosphates in plant cell signaling. Adv. Exp. Med. Biol. **991:** 141–157.

Gilroy, S., Read, N.D., and Trewavas, A.J. (1990). Elevation of cytoplasmic calcium by caged calcium or caged inositol triphosphate initiates stomatal closure. Nature **346:** 769–771.

Han, S., Tang, R., Anderson, L.K., Woerner, T.E., and Pei, Z.M. (2003). A cell surface receptor mediates extracellular Ca^{2+} sensing in guard cells. Nature **425:** 196–200.

Hanke, D.E., Parmar, P.N., Caddick, S.E., Green, P., and Brearley, C.A. (2012). Synthesis of inositol phosphate ligands of plant hormone-receptor complexes: pathways of inositol hexakisphosphate turnover. Biochem. J. **444:** 601–609.

Howe, G.A., and Jander, G. (2008). Plant immunity to insect herbivores. Annu. Rev. Plant Biol. **59:** 41–66.

Katoh, K., Kuma, K., Toh, H., and Miyata, T. (2005). MAFFT version 5: improvement in accuracy of multiple sequence alignment. Nucleic Acids Res. **33:** 511–518.

Katsir, L., Schilmiller, A.L., Staswick, P.E., He, S.Y., and Howe, G.A. (2008). COI1 is a critical component of a receptor for jasmonate and the bacterial virulence factor coronatine. Proc. Natl. Acad. Sci. USA **105:** 7100–7105.

Keeling, P., Leander, B.S., and Simpson, A. (2009). Eukaryotes. Eukaryota: Organisms with nucleated cells. In The Tree of Life Project, http://tolweb.org/Eukaryotes/3/2009.10.28.

Kemmerling, B., et al. (2007). The BRI1-associated kinase 1, BAK1, has a brassinolide-independent role in plant cell-death control. Curr. Biol. **17:** 1116–1122.

Knight, H., Trewavas, A.J., and Knight, M.R. (1997). Calcium signalling in *Arabidopsis thaliana* responding to drought and salinity. Plant J. **12:** 1067–1078.

Kumar, S., Skjaeveland, A., Orr, R.J.S., Enger, P., Ruden, T., Mevik, B.H., Burki, F., Botnen, A., and Shalchian-Tabrizi, K. (2009). AIR: A batch-oriented web program package for construction of supermatrices ready for phylogenomic analyses. BMC Bioinformatics **10:** 357.

Lemtiri-Chlieh, F., MacRobbie, E.A., and Brearley, C.A. (2000). Inositol hexakisphosphate is a physiological signal regulating the K^+-inward rectifying conductance in guard cells. Proc. Natl. Acad. Sci. USA **97:** 8687–8692.

Lin, H., Fridy, P.C., Ribeiro, A.A., Choi, J.H., Barma, D.K., Vogel, G., Falck, J.R., Shears, S.B., York, J.D., and Mayr, G.W. (2009). Structural analysis and detection of biological inositol pyrophosphates reveal that the family of VIP/diphosphoinositol pentakisphosphate kinases are 1/3-kinases. J. Biol. Chem. **284:** 1863–1872.

Liu, H.T., Gao, F., Cui, S.J., Han, J.L., Sun, D.Y., and Zhou, R.G. (2006). Primary evidence for involvement of IP3 in heat-shock signal transduction in Arabidopsis. Cell Res. **16:** 394–400.

Losito, O., Szijgyarto, Z., Resnick, A.C., and Saiardi, A. (2009). Inositol pyrophosphates and their unique metabolic complexity: analysis by gel electrophoresis. PLoS ONE **4:** e5580.

Menniti, F.S., Miller, R.N., Putney, J.W., Jr., and Shears, S.B. (1993). Turnover of inositol polyphosphate pyrophosphates in pancreatoma cells. J. Biol. Chem. **268:** 3850–3856.

Mosblech, A., Thurow, C., Gatz, C., Feussner, I., and Heilmann, I. (2011). Jasmonic acid perception by COI1 involves inositol polyphosphates in *Arabidopsis thaliana*. Plant J. **65:** 949–957.

Mosblech, A., König, S., Stenzel, I., Grzeganek, P., Feussner, I., and Heilmann, I. (2008). Phosphoinositide and inositolpolyphosphate signalling in defense responses of *Arabidopsis thaliana* challenged by mechanical wounding. Mol. Plant **1:** 249–261.

Mulugu, S., Bai, W., Fridy, P.C., Bastidas, R.J., Otto, J.C., Dollins, D.E., Haystead, T.A., Ribeiro, A.A., and York, J.D. (2007). A conserved family of enzymes that phosphorylate inositol hexakisphosphate. Science **316:** 106–109.

Munnik, T., and Vermeer, J.E. (2010). Osmotic stress-induced phosphoinositide and inositol phosphate signalling in plants. Plant Cell Environ. **33:** 655–669.

Munnik, T., and Nielsen, E. (2011). Green light for polyphosphoinositide signals in plants. Curr. Opin. Plant Biol. **14:** 489–497.

Murphy, A.M., Otto, B., Brearley, C.A., Carr, J.P., and Hanke, D.E. (2008). A role for inositol hexakisphosphate in the maintenance of basal resistance to plant pathogens. Plant J. **56:** 638–652.

Onnebo, S.M., and Saiardi, A. (2009). Inositol pyrophosphates modulate hydrogen peroxide signalling. Biochem. J. **423:** 109–118.

Osada, S., Kageyama, K., Ohnishi, Y., Nishikawa, J., Nishihara, T., and Imagawa, M. (2012). Inositol phosphate kinase Vip1p interacts with histone chaperone Asf1p in *Saccharomyces cerevisiae*. Mol. Biol. Rep. **39:** 4989–4996.

Padmanabhan, U., Dollins, D.E., Fridy, P.C., York, J.D., and Downes, C.P. (2009). Characterization of a selective inhibitor of inositol hexakisphosphate kinases: use in defining biological roles and metabolic relationships of inositol pyrophosphates. J. Biol. Chem. **284:** 10571–10582.

Perera, I.Y., Hung, C.Y., Moore, C.D., Stevenson-Paulik, J., and Boss, W.F. (2008). Transgenic Arabidopsis plants expressing the type 1 inositol 5-phosphatase exhibit increased drought tolerance and altered abscisic acid signaling. Plant Cell **20:** 2876–2893.

Pieterse, C.M., and Dicke, M. (2007). Plant interactions with microbes and insects: from molecular mechanisms to ecology. Trends Plant Sci. **12:** 564–569.

Pieterse, C.M., Van der Does, D., Zamioudis, C., Leon-Reyes, A., and Van Wees, S.C. (2012). Hormonal modulation of plant immunity. Annu. Rev. Cell Dev. Biol. **28:** 489–521.

Pöhlmann, J., Risse, C., Seidel, C., Pohlmann, T., Jakopec, V., Walla, E., Ramrath, P., Takeshita, N., Baumann, S., Feldbrügge, M., Fischer, R., and Fleig, U. (2014). The Vip1 inositol polyphosphate kinase family regulates polarized growth and modulates the microtubule cytoskeleton in fungi. PLoS Genet. **10:** e1004586.

Rao, F., et al. (2014). Inositol pyrophosphates mediate the DNA-PK/ATM-p53 cell death pathway by regulating CK2 phosphorylation of Tti1/Tel2. Mol. Cell **54:** 119–132.

Safrany, S.T., Caffrey, J.J., Yang, X., Bembenek, M.E., Moyer, M.B., Burkhart, W.A., and Shears, S.B. (1998). A novel context for the 'MutT' module, a guardian of cell integrity, in a diphosphoinositol polyphosphate phosphohydrolase. EMBO J. **17:** 6599–6607.

Saiardi, A., Caffrey, J.J., Snyder, S.H., and Shears, S.B. (2000a). The inositol hexakisphosphate kinase family. Catalytic flexibility and function in yeast vacuole biogenesis. J. Biol. Chem. **275:** 24686–24692.

Saiardi, A., Caffrey, J.J., Snyder, S.H., and Shears, S.B. (2000b). Inositol polyphosphate multikinase (ArgRIII) determines nuclear mRNA export in *Saccharomyces cerevisiae*. FEBS Lett. **468:** 28–32.

Saiardi, A., Nagata, E., Luo, H.R., Snowman, A.M., and Snyder, S.H. (2001). Identification and characterization of a novel inositol hexakisphosphate kinase. J. Biol. Chem. **276:** 39179–39185.

Sheard, L.B., et al. (2010). Jasmonate perception by inositol-phosphate-potentiated COI1-JAZ co-receptor. Nature **468:** 400–405.

Shears, S.B. (2009). Diphosphoinositol polyphosphates: metabolic messengers? Mol. Pharmacol. **76:** 236–252.

Stamatakis, A. (2006a). RAxML-VI-HPC: maximum likelihood-based phylogenetic analyses with thousands of taxa and mixed models. Bioinformatics **22:** 2688–2690.

Stamatakis, A. (2006b). Phylogenetic models of rate heterogeneity: A high performance computing perspective. In 20th International

Parallel and Distributed Processing Symposium (IPDPS), 10.1109/IPDPS.2006.1639535.

Stamatakis, A., Hoover, P., and Rougemont, J. (2008). A rapid bootstrap algorithm for the RAxML Web servers. Syst. Biol. **57:** 758–771.

Stephens, L.R., Hawkins, P.T., Stanley, A.F., Moore, T., Poyner, D.R., Morris, P.J., Hanley, M.R., Kay, R.R., and Irvine, R.F. (1991). Myo-inositol pentakisphosphates. Structure, biological occurrence and phosphorylation to myo-inositol hexakisphosphate. Biochem. J. **275:** 485–499.

Stevenson-Paulik, J., Bastidas, R.J., Chiou, S.T., Frye, R.A., and York, J.D. (2005). Generation of phytate-free seeds in Arabidopsis through disruption of inositol polyphosphate kinases. Proc. Natl. Acad. Sci. USA **102:** 12612–12617.

Streb, H., Irvine, R.F., Berridge, M.J., and Schulz, I. (1983). Release of Ca^{2+} from a nonmitochondrial intracellular store in pancreatic acinar cells by inositol-1,4,5-trisphosphate. Nature **306:** 67–69.

Szijgyarto, Z., Garedew, A., Azevedo, C., and Saiardi, A. (2011). Influence of inositol pyrophosphates on cellular energy dynamics. Science **334:** 802–805.

Tan, X., Calderon-Villalobos, L.I., Sharon, M., Zheng, C., Robinson, C.V., Estelle, M., and Zheng, N. (2007). Mechanism of auxin perception by the TIR1 ubiquitin ligase. Nature **446:** 640–645.

Thines, B., Katsir, L., Melotto, M., Niu, Y., Mandaokar, A., Liu, G., Nomura, K., He, S.Y., Howe, G.A., and Browse, J. (2007). JAZ repressor proteins are targets of the SCF(COI1) complex during jasmonate signalling. Nature **448:** 661–665.

Van Wees, S.C., Van Pelt, J.A., Bakker, P.A., and Pieterse, C.M. (2013). Bioassays for assessing jasmonate-dependent defenses triggered by pathogens, herbivorous insects, or beneficial rhizobacteria. Methods Mol. Biol. **1011:** 35–49.

Verhage, A., Vlaardingerbroek, I., Raaymakers, C., Van Dam, N.M., Dicke, M., Van Wees, S.C., and Pieterse, C.M. (2011). Rewiring of the jasmonate signaling pathway in Arabidopsis during insect herbivory. Front. Plant Sci. **2:** 47.

Vos, I.A., Verhage, A., Schuurink, R.C., Watt, L.G., Pieterse, C.M.J., and Van Wees, S.C.M. (2013). Onset of herbivore-induced resistance in systemic tissue primed for jasmonate-dependent defenses is activated by abscisic acid. Front. Plant Sci. **4:** 539.

Wang, H., Falck, J.R., Hall, T.M., and Shears, S.B. (2012). Structural basis for an inositol pyrophosphate kinase surmounting phosphate crowding. Nat. Chem. Biol. **8:** 111–116.

Wang, Y., Chu, Y.J., and Xue, H.W. (2012). Inositol polyphosphate 5-phosphatase-controlled Ins(1,4,5)P3/Ca^{2+} is crucial for maintaining pollen dormancy and regulating early germination of pollen. Development **139:** 2221–2233.

Wang, Y., Lin, W.H., Chen, X., and Xue, H.W. (2009). The role of Arabidopsis 5PTase13 in root gravitropism through modulation of vesicle trafficking. Cell Res. **19:** 1191–1204.

Wundenberg, T., and Mayr, G.W. (2012). Synthesis and biological actions of diphosphoinositol phosphates (inositol pyrophosphates), regulators of cell homeostasis. Biol. Chem. **393:** 979–998.

Yan, J., Li, H., Li, S., Yao, R., Deng, H., Xie, Q., and Xie, D. (2013). The Arabidopsis F-box protein CORONATINE INSENSITIVE1 is stabilized by SCFCOI1 and degraded via the 26S proteasome pathway. Plant Cell **25:** 486–498.

Yang, Z. (1993). Maximum-likelihood estimation of phylogeny from DNA sequences when substitution rates differ over sites. Mol. Biol. Evol. **10:** 1396–1401.

York, J.D. (2006). Regulation of nuclear processes by inositol polyphosphates. Biochim. Biophys. Acta **1761:** 552–559.

Zhang, J., et al. (2011). Inositol trisphosphate-induced Ca^{2+} signaling modulates auxin transport and PIN polarity. Dev. Cell **20:** 855–866.

VIH2 Regulates the Synthesis of Inositol Pyrophosphate InsP$_8$ and Jasmonate-Dependent Defenses in Arabidopsis

Debabrata Laha, Philipp Johnen, Cristina Azevedo, Marek Dynowski, Michael Weiß, Samanta Capolicchio, Haibin Mao, Tim Iven, Merel Steenbergen, Marc Freyer, Philipp Gaugler, Marília K.F. de Campos, Ning Zheng, Ivo Feussner, Henning J. Jessen, Saskia C.M. Van Wees, Adolfo Saiardi and Gabriel Schaaf

This information is current as of February 8, 2019

Supplemental Data	/content/suppl/2015/04/08/tpc.114.135160.DC1.html
References	This article cites 75 articles, 23 of which can be accessed free at: /content/27/4/1082.full.html#ref-list-1
Permissions	https://www.copyright.com/ccc/openurl.do?sid=pd_hw1532298X&issn=1532298X&WT.mc_id=pd_hw1532298X
eTOCs	Sign up for eTOCs at: http://www.plantcell.org/cgi/alerts/ctmain
CiteTrack Alerts	Sign up for CiteTrack Alerts at: http://www.plantcell.org/cgi/alerts/ctmain
Subscription Information	Subscription Information for *The Plant Cell* and *Plant Physiology* is available at: http://www.aspb.org/publications/subscriptions.cfm